ON THE ESTIMATION OF SCALE OF FLUCTUATION IN GEOSTATISTICS

M. Lloret-Cabot[1,2], G.A. Fenton[2,3], M.A. Hicks[2]

[1] *Centre for Geotechnical and Materials Modelling, University of Newcastle, Newcastle, Australia.*

[2] *Department of Geoscience and Engineering, Delft University of Technology, Delft, The Netherlands.*

[3] *Department of Engineering Mathematics, Dalhousie University, Halifax, Canada.*

ON THE ESTIMATION OF SCALE OF FLUCTUATION IN GEOSTATISTICS

Describing how soil properties vary spatially is of particular importance in stochastic analyses of geotechnical problems, because spatial variability has a significant influence on local material and global geotechnical response. In particular, the scale of fluctuation θ is a key parameter in the correlation model used to represent the spatial variability of a site through a random field. It is therefore of fundamental importance to accurately estimate θ in order to best model the actual soil heterogeneity.

In this paper, two methodologies are investigated to assess their abilities to estimate the vertical and horizontal scales of fluctuation of a particular site using in situ Cone Penetration Test (CPT) data. The first method belongs to the family of more traditional approaches, which are based on best fitting a theoretical correlation model to available CPT data. The second method involves a new strategy which combines information from conditional random fields with the traditional approach. Both methods are applied to a case study involving the estimation of θ at three two-dimensional sections across a site and the results obtained show general agreement between the two methods, suggesting a similar level of accuracy between the new and traditional approaches. However, in order to further assess the relative accuracy of estimates provided by each method, a second numerical analysis is proposed. The results confirm the general consistency observed in the case study calculations, particularly in the vertical direction where a large amount of data are available. Interestingly, for the horizontal direction, where data are typically scarce, some additional improvement in terms of relative error is obtained with the new approach.

Keywords: spatial variability; random fields; soil heterogeneity; characterization of soil/rock variability; geostatistics

1. Introduction

This paper compares the performance of two different methods to estimate the vertical and horizontal scales of fluctuation using in situ Cone Penetration Test (CPT) data from a particular test site. The first method will be referred to as Approach A and is based on

more conventional (or classical) approaches. The second method will be referred to as Approach B and involves a new strategy which combines information from conditional random fields with the traditional approach. To illustrate and assess their relative performance, both strategies are applied to a case study and the results are evaluated. The goal of the paper is to answer the question: Are conventional techniques for estimating the correlation length as good as they can be, or is there the possibility for improvement?

The scale of fluctuation θ is a convenient measure for describing the spatial variability of a soil property in a random field. It is a measure of the distance within which points are significantly correlated (Vanmarcke, 1984). Points separated by a larger distance than θ will show little correlation, and practically no correlation will be observed when points are separated by a significantly larger distance than θ. This relationship between soil property values and relative distances is contained within the correlation model, which is a function of the lag τ (i.e. distance between points) and the scale of fluctuation θ. Some common correlation models are summarized in Table 1, including the Gaussian model, the triangular model, the spherical model and the Markov correlation model used here. In each of these models, small values of θ imply that the correlation function falls off rapidly to zero with increasing τ (i.e. the correlation between two points becomes rapidly smaller), which leads to rougher random fields. In the limit, as $\theta \rightarrow 0$, all points in the domain become uncorrelated and the field becomes infinitely rough. At the other extreme, for increasing values of θ the soil property field becomes smoother, or, in other words, the field shows less variability converging to a uniform field when $\theta \rightarrow \infty$.

The correlation model is a fundamental ingredient in the stochastic analyses of geotechnical problems, not only because it describes how the soil property values vary

spatially throughout the geometrical domain, but, more importantly, because the spatial variation itself has a significant influence on the response of the geotechnical structure. This is of special interest, given that random fields are typically used to model soil heterogeneity (i.e. inherent variability), in advanced stochastic analyses (Fenton, 1999; Fenton and Griffiths, 2003; Hicks and Onisiphorou, 2005; Fenton and Griffiths, 2005; Griffiths et al., 2009; Hicks and Spencer, 2010; Cassidy et al., 2013).

Perhaps due to the complexity associated with the modelling of soil heterogeneity, however, little research has been done to accurately describe its nature and this has typically led to inherent variability being one of the primary sources of uncertainty in stochastic analyses in geotechnical engineering (Fenton, 1999; Phoon and Kulhawy, 1999). The scale of fluctuation, in particular, plays a key role in the description of soil variability at a site. It is therefore crucial to estimate accurate values of the vertical and horizontal scales of fluctuation in order to obtain more realistic responses of the geotechnical structure when using advanced probabilistic approaches. Indeed, investigating scales of fluctuation from in situ data is a subject of general interest in geotechnical engineering, particularly with respect to the horizontal plane. This is because, although a number of investigations appear in the literature for the vertical scale of fluctuation (e.g. Fenton, 1999; Hicks and Onisiphorou, 2005), there is still rather limited information for the horizontal direction. This is in spite of the fact that researchers have demonstrated that the ratio of the horizontal and vertical scales of fluctuation is an important consideration in geotechnical computations (Hicks and Samy, 2002; Hicks and Onisiphorou, 2005; Hicks and Spencer, 2010).

The aim of both strategies considered here, for the estimation of the vertical and horizontal scales of fluctuation, is to minimise the error between the assumed *theoretical* correlation model and the *estimated* (or *experimental*) correlation structure

(the latter being estimated from CPT data from the site being investigated). In order to explore the performance of each method, an extensive set of CPT data, from an artificial sand island constructed offshore to provide a temporary platform for oil and gas exploration, is considered. In particular, CPT measurements from three vertical cross-sections through the sand fill core of the island are investigated. In Approach A (the first and more conventional approach considered in this study), the CPT data are solely used to estimate the experimental correlation model in the horizontal and vertical directions for each section, whereas, in Approach B, the CPT data are also used to generate a conditional random field from which the experimental correlation model is estimated. It is believed that the use of a conditioned random field makes more complete use of the available site information, particularly when the data are scarce, and so should provide a means of checking the accuracy of conventional estimation techniques. Approach B starts by using the CPTs to statistically describe the tip resistances q_c of the sand fill core of the island. The obtained statistics are then used to generate a 2-D random field of q_c, which is later constrained (conditioned) at the CPT locations. This new conditional random field is used to estimate the experimental correlation functions for the site (in the horizontal and vertical directions), which are then compared to the respective horizontal and vertical theoretical correlation models to find the estimated values of θ in each direction. Finally, the conventional estimation techniques that are used in Approach A (and which operate on the data directly) are employed to obtain another set of correlation length estimates. The two sets of estimates are then compared to assess the relative accuracy of the two approaches.

2. APPROACHES USED TO ESTIMATE θ

Various methods are available to estimate the scale of fluctuation. The simplest approach is probably to estimate θ by best fitting the theoretical correlation model to the

experimental correlation function (Vanmarcke, 1977; Campanella et al., 1987; DeGroot and Baecher, 1993; Fenton, 1999; Baecher and Christian, 2003; Wackernagel, 2003; Uzielli et al., 2005, Fenton and Griffiths, 2008). Vanmarcke (1984) and Wickremesinghe and Camapanella (1993) proposed an alternative method, based on the concept of variance function discussed in Vanmarcke (1977), which has been used in several studies (Jaksa et al., 1993; Hicks and Onisiphorou, 2005; Lloret et al., 2012; Lloret-Cabot et al., 2013). Other techniques, combining random field theory with conventional approaches, have also been recently proposed (Kim and Santamarina, 2008; Zhang et al., 2008; Dasaka and Zhang, 2012).

The two approaches used here to estimate θ are based on the concept of best fitting the theoretical correlation model $\rho(\tau)$,

$$\rho(\tau) = \exp\left\{\frac{-2|\tau|}{\theta}\right\} \tag{1}$$

to the estimated correlation function $\hat{\rho}(\tau)$

$$\hat{\rho}(\tau_j) = \frac{1}{\hat{\sigma}^2(k-j)} \sum_{i=1}^{k-j+1} (X_i - \hat{\mu})(X_{i+j} - \hat{\mu}) \tag{2}$$

where $\hat{\mu}$ and $\hat{\sigma}$ are the estimated mean and standard deviation from the in situ CPT data and $\tau_j = j\Delta\tau$, with $j = 1, 2, \ldots, k$, and k being the number of observations. Note that, for the estimator given by Equation (2), it is desirable that the data be equi-spaced (Fenton and Griffiths, 2008) at spacing $\Delta\tau$.

Considering now the following error measure,

$$E = \sum_{j=1}^{k} \left(\hat{\rho}(\tau_j) - \rho(\tau_j)\right)^2 \tag{3}$$

one may compute the value of θ that minimizes E by finding a root to the following expression:

$$\frac{\partial E}{\partial \theta} = -\sum_{j=1}^{k} 2\frac{\tau_j}{\theta^2}\left(\hat{\rho}(\tau_j) - \exp\left\{\frac{-2|\tau_j|}{\theta}\right\}\right)\exp\left\{\frac{-2|\tau_j|}{\theta}\right\} \quad (4)$$

which can be expressed as:

$$\sum_{j=1}^{k} \tau_j\left(\hat{\rho}(\tau_j) - \exp\left\{\frac{-2|\tau_j|}{\theta}\right\}\right)\exp\left\{\frac{-2|\tau_j|}{\theta}\right\} = 0 \quad (5)$$

For simplicity, the correlation model $\rho(\tau)$ is assumed to have the exponential form shown in Equation (1), but alternatives such as those summarized in Table 1 are also possible (Fenton and Griffiths, 2008).

In essence, both approaches presented in this paper use the same idea of minimising the error between the assumed theoretical and experimental correlation models. The main difference between Approach A (the conventional approach) and Approach B (the new method proposed) is how the experimental correlation model is estimated. In Approach A, the experimental correlation model $\hat{\rho}(\tau)$ is simply estimated using Equation (2) with the CPT data directly, whereas, in Approach B, $\hat{\rho}(\tau)$ is estimated from the generated conditional random field. A detailed description of how the experimental correlation model is estimated when using Approach B is summarised next.

The algorithm is equivalent in the vertical and horizontal directions and comprises the following steps. Further details are given in the next section where the algorithm is applied to a case study.

i. Find the linear depth trend of q_c in each CPT considered and remove it from the data. Calculate the standard deviation σ_{res} of the de-trended tip resistances for each CPT. Normalize each individual set of de-trended tip resistances by dividing by the corresponding standard deviation σ_{res}. Each individual CPT is de-trended and normalized in order to produce a standard normal field ($\hat{\mu}$ = 0, $\hat{\sigma}$ = 1).

ii. The correlation function is estimated separately in the vertical and horizontal directions. For the vertical direction, estimate the correlation function for each CPT, using Equation (2) with the normalized de-trended tip resistances. Then estimate the *average* vertical correlation function from the individual vertical correlation functions. For the horizontal direction, estimate the horizontal correlation function for different depths, by using Equation (2) with the corresponding normalized de-trended CPT tip resistances for different horizontal lags. Then average the correlation functions with respect to depth to get the estimated *average* horizontal correlation function for different lags.

Find the initial estimates of the vertical and horizontal scales of fluctuation $\left\{\hat{\theta}_v, \hat{\theta}_h\right\}_0$, by using Equation (5) with the averaged correlation functions (this is Approach A). Set i = 1.

iii. Generate the ith standard normal random field of normalized de-trended q_c based on the statistics found in (i) and (ii), assuming that the normalized de-trended tip resistances can be represented by a standard normal distribution function.

iv. Constrain the ith random field computed in (iii) at the locations of the CPT measurements, i.e. resulting in the ith conditional random field. A brief

description of the implemented conditional approach is given in the following section.

v. Using Equation (2), with $\hat{\mu}$ = 0 and $\hat{\sigma}$ = 1, compute $\hat{\rho}_i(\tau)$ from the *i*th conditional random field calculated in (iv).

vi. Use $\hat{\rho}_i(\tau)$, computed in (v), to find the root of Equation (5) in the vertical and horizontal directions, giving $\left\{\hat{\theta}_v, \hat{\theta}_h\right\}_i$.

vii. Update $i = i+1$ and go to (iii), repeating the process until the number of simulations performed is *n*.

viii. The final estimates of the vertical and horizontal scales of fluctuation are the average values computed in (vi) of $\left\{\hat{\theta}_v, \hat{\theta}_h\right\}_i$, from i = 1 to n, where n is the number of simulations performed.

The fact that each conditional random field is constrained at the known CPT measurements implies that the field contains *true* information of the actual soil variability at the site and, therefore, is likely to provide a more realistic estimation of the correlation function and thereby a better estimate of the scales of fluctuation than the initial estimates given in (ii) when using the conventional approach (i.e. Approach A).

2.1 Conditional random fields

The (unconditioned) random fields involved in the conditional Approach B are generated using the Local Average Subdivision (LAS) method proposed by Fenton and Vanmarcke (1990). The LAS method requires a probability density function (pdf) with its statistics (mean μ and standard deviation σ) and a scale of fluctuation θ. As mentioned earlier, the statistical information for q_c in this paper is estimated from the available field data at each 2-D section investigated.

The generated 2-D random fields are then constrained (i.e. conditioned) at the locations of the actual CPT measurements. The conditioning approach follows the work of van den Eijnden and Hicks (2011), which applied the Kriging interpolation technique (Krige, 1951; Cressie, 1990; Wackernagel, 2003; Fenton and Griffiths, 2008) to give the best linear unbiased estimate of a random field between known data. In essence, the Kriging method estimates a random field Z at desired locations $\mathbf{x}$, from a linear combination of known values of Z at m observations points $\mathbf{x}_\alpha$. The Kriged interpolation of Z at $\mathbf{x}$ (i.e. $Z^*(\mathbf{x})$) can be expressed as:

$$Z^*(\mathbf{x}) = \sum_{\alpha=1}^{m} \lambda_\alpha Z(\mathbf{x}_\alpha) \quad \text{with} \quad \sum_{\alpha=1}^{m} \lambda_\alpha = 1 \tag{6}$$

where λ_α are the m unknown weights that are determined by minimising the variance of the difference between the Kriged field Z^* and the original field Z (Wackernagel, 2003). Kriging can be used to condition the random field at the known (conditioning) points, as summarised in the following four steps (Journel and Huijbregts, 1978; van den Eijnden and Hicks, 2011).

i. Generate an unconditional random field $Z_s(\mathbf{x})$ with known point statistics and correlation structure, and extract the values of $Z_s(\mathbf{x})$ at the locations $\mathbf{x}_\alpha$ (i.e. $Z_s(\mathbf{x}_\alpha)$ for $\alpha = 1$ to m).
ii. Generate an initial interpolated field $Z_0^*(\mathbf{x})$ by Kriging, using the known (conditioning) measurements $Z(\mathbf{x}_\alpha)$ at the locations $\mathbf{x}_\alpha$ and according to the assumed correlation model.
iii. Generate $Z_s^*(\mathbf{x})$ by Kriging using the values $Z_s(\mathbf{x}_\alpha)$ calculated in step (i).
iv. Calculate the conditional random field $Z_{cs}(\mathbf{x})$ as:

$$Z_{cs}(\mathbf{x}) = \left(Z_s(\mathbf{x}) - Z_s^*(\mathbf{x})\right) + Z_0^*(\mathbf{x}) \tag{7}$$

3. Application to a real case study

Numerous artificial islands were constructed during the 1970s and 80s in the Canadian Beaufort Sea, to provide temporary structures for hydrocarbon exploration. One type of island used caisson technology to reduce the required fill volumes (Hicks and Smith, 1988). Figure 1a shows that this type of island incorporated two main sand fills: (a) an underwater berm on which the caisson was founded; and (b) the body of the island structure (referred to as the core). This paper investigates data from one such island, Tarsuit P-45. In particular, eighteen CPTs from the site are used here to statistically describe the tip resistances q_c of the sand fill core, these CPTs lying along three straight lines in a plan view of the core, as shown in Figure 1b. The number of CPTs aligned along the first, second and third sections are seven, six and five, respectively, and each line of CPTs indicates the soil variability for that 2-D section (denoted as AA', BB' and CC' in Figure 1b). For simplicity, the same geometry of 50 m length by 5.5 m depth is considered for all three sections (see Figure 6). Note that, in order to be consistent in the geometry of all three sections analysed, all CPT measurements investigated are located in a depth range of 1 m to 6.5 m (see Figure 2).

The statistics obtained for each section are used to generate a 2-D random field of normalized de-trended q_c, which is later constrained (conditioned) at the corresponding CPT locations. The statistical characterization of the sand fill core of Tarsuit P-45 follows previous research by Wong (2004) and is only briefly summarised below.

Figure 2 shows the CPT tip resistance data for each section investigated. In the plots, the thin broken lines indicate q_c values for individual CPTs profiles, whereas the thicker straight dashed lines indicate the average linear mean trend between 1 m to 6.5 m. The mean and standard deviation of q_c are calculated separately for each section to

give the average values summarized in Table 2. Inspection of Figure 2 shows that the average linear depth trend is very similar for the three sections, indicating a similar underlying depth-dependency of the q_c values. This is also illustrated in Table 2, where the average slope and intercept of the linear trend identified in each section are similar.

A standard normal distribution is used to represent the normalized de-trended cone tip resistances of the Tarsuit P-45 core. Figure 3 shows the histograms based on all data from the CPTs involved in the section analysed, as well as the fitted distribution. Inspection of this figure shows that, for the three sections investigated, the variation of normalized de-trended tip resistance is reasonably well represented by a standard normal distribution. On the right-hand-side of this figure, the normalized de-trended CPT data used for each histogram are plotted.

The estimates of the vertical and horizontal scales of fluctuation when using Approach A are summarized in Table 3. Note that these are the initial guesses used in Approach B when using the conditional random field. Figures 4 and 5 show the estimated correlation functions from Approach A as dashed lines, for the vertical and horizontal directions, respectively. Note that the correlation estimates become increasingly variable as the lag increases, due to there being fewer data pairs available with larger lags (Fenton and Griffiths, 2008). This is particularly evident for section CC', as well as for later simulations in the paper. The theoretical correlation function (using the estimated value of θ from Approach A) is represented by a thick solid line. Inspection of Figure 4 shows that very similar initial estimates of θ_v are obtained for the three sections (see also Table 3), indicating that this part of the sand fill island core exhibits a consistent vertical variability of q_c. However, as shown in Figure 5, this is not apparent for the horizontal direction, where the differences between initial estimates for

θ_h are much larger and range from 1.69 m to 13.69 m. Although this large range of values may in part be to actual soil variation, the scarcity of data will also be a factor.

A 2-D standard normal random field is generated for each section analysed, using the initial values of the scales of fluctuation obtained from Approach A (see Table 3). Each generated random field is subsequently conditioned at the observed CPT locations by the CPT data, yielding conditional random fields similar to those illustrated in Figure 6. Note that, in the plots of Figure 6, the scales in the vertical and horizontal directions are not the same.

From each of the conditional random fields, it is straightforward to estimate the corresponding correlation structure by using Equation (2), which can then be compared against the theoretical correlation model in each direction in order to estimate the value of θ (i.e. as a root of Equation (5)). The average of the vertical and horizontal scales of fluctuation, over the total number of realizations *n*, gives the estimated values of θ_v and θ_h when using Approach B (see Table 3). For the analyses presented in this section, the total number of realizations considered is n = 100. Figures 7 and 8 illustrate the estimated correlation function for the vertical and horizontal directions, respectively, for all realizations when using Approach B. In the figures, the thicker solid line indicates the theoretical correlation structure $\rho(\tau)$ using the estimated value of θ; the thinner fine lines indicate each of the estimated $\hat{\rho}_i(\tau)$ and the thick dashed line indicates the average of all the estimated $\hat{\rho}_i(\tau)$.

Overall, Figure 7 shows that the theoretical correlation structure is a satisfactory fit to $\hat{\rho}(\tau)$ for the three sections considered. The results for section AA' in the vertical direction (Figure 7a) suggest an average of θ_v = 0.41 m, while for section BB' (Figure 7b) the average is θ_v = 0.42 m, and for section CC' (Figure 7c) the average is θ_v = 0.40

m. The results suggest that the variability in the vertical direction is very consistent across the sections considered (Table 3).

A larger variation is observed in Figure 8 when looking at the estimated horizontal correlation functions for sections AA', BB' and CC'. Section AA' shows an average of θ_h = 1.82 m, whereas sections BB' and CC' give, respectively, θ_h = 5.60 m and θ_h = 15.86 m (Table 3). A possible explanation for these differences is that less CPT measurements (i.e. *true* data points) are available in the horizontal direction. Also, the horizontal distance between CPTs is relatively large compared to the obtained θ_h (see Figures 1 and 5), resulting in only a few *true* data points over the initial part of the estimated correlation structure ($\tau_h < \theta_h$), which is, indeed, the most relevant part of the curve when estimating the θ of the correlation model. Conversely, in the vertical direction, *true* measurements are available every 0.02 m (i.e. the vertical distance between each CPT measurement) and this distance is, conveniently, significantly smaller than the obtained θ_v. This is well illustrated in Figure 4, where many *true* data points are available in the relevant part of the curve (i.e. $\tau_v < \theta_v$), providing more confidence in the estimated value of θ_v than that of θ_h obtained for the horizontal case.

4. Accuracy assessment

A fundamental part of the investigation is to assess the accuracy of the two approaches used to estimate θ. This section aims to address this issue by proposing a numerical strategy and applying it to a fictitious site with the same geometry as analysed in the previous case study. A 2-D random field of normalized de-trended tip resistances is generated with known or *true* statistics (μ = 0; σ = 1, θ_v = 0.5 m and θ_h = 5 m). From this fictitious site 7 CPTs are extracted at the same locations given in Figure 1b for section AA'. The seven CPTs are then used to calculate the statistics of q_c in the same manner as explained earlier for the case study. Approach B detailed in the previous

section is then applied to find estimated values of the vertical and horizontal scales of fluctuation. A number of pairs $\left\{\hat{\theta}_v, \hat{\theta}_h\right\}_j$ are obtained by repeating this process from j = 1 to k, i.e. over k realizations of the random field of normalized de-trended tip resistances. In order to assess the accuracy of the new approach for estimating θ, the statistics from all pairs $\left\{\hat{\theta}_v, \hat{\theta}_h\right\}_j$ can be compared against the *true* values of θ $\left\{\theta_v, \theta_h\right\}$ used to generate the initial random tip resistance fields. Similarly, the initial estimated pairs of vertical and horizontal scales of fluctuation $\left\{\hat{\theta}_v, \hat{\theta}_h\right\}_{0,j}$, obtained using Approach A, can be used to assess the accuracy of the conventional approach. The steps for assessing the relative accuracy of the conventional and proposed new approach are summarized as follows:

i. Set j = 1.

ii. Generate a generic (non-conditional) random field of tip resistances with known statistics ($\mu = 0, \sigma = 1$, θ_v and θ_h), assuming a standard normal distribution.

iii. Extract l CPTs at the appropriate locations.

iv. Using these l CPTs, estimate the statistics $\left\{\hat{\theta}_v, \hat{\theta}_h\right\}_{0,j}$ in the same manner as described in the case study (Approach A).

v. Estimate $\left\{\hat{\theta}_v, \hat{\theta}_h\right\}_j$ using Approach B:

   (a) Generate the i*th* standard normal random field of normalized de-trended q_c based on the statistics found in (iv). Set i = 1.

(b) Constrain the i*th* random field computed in (a) at the locations of the CPT measurements from (iii), resulting in the i*th* conditional random field.

(c) Using Equation (2) with $\hat{\mu}$ = 0 and $\hat{\sigma}$ = 1, compute $\hat{\rho}_i(\tau)$ from the *i*th conditional random field calculated in (b).

(d) Use $\hat{\rho}_i(\tau)$, computed in (c), to find the root of Equation (5) in the vertical and horizontal directions, giving $\left\{\hat{\theta}_v, \hat{\theta}_h\right\}_i$.

(e) Update $i = i+1$ and go to (a), repeating the process until the number of simulations performed, *n*.

(f) The final estimates of the vertical and horizontal scales of fluctuation, $\left\{\hat{\theta}_v, \hat{\theta}_h\right\}_j$, are the average values computed in (d) of $\left\{\hat{\theta}_v, \hat{\theta}_h\right\}_i$ from $i = 1$ to *n*, where *n* is the number of simulations performed.

vi. Update $j = j+1$ and go to (ii), repeating the process until *k* realizations.

vii. Compare the output pairs of values, $\left\{\hat{\theta}_v, \hat{\theta}_h\right\}_{0,j}$ and $\left\{\hat{\theta}_v, \hat{\theta}_h\right\}_j$, against the *true* θ_v and θ_h used in (ii) to assess the accuracy of the classical and new approaches.

The above steps for assessing the accuracy of the approaches used for the determination of the scales of fluctuation are applied to section AA' (Figure 1b). Table 4 summarizes the relevant information obtained from the 30, i.e. $k = 30$, random fields generated in the proposed algorithm to assess the accuracy of Approaches A and B. In Approach B, i.e. steps (a) to (f), the number of simulations considered to estimate the final statistics is $n = 35$. The results presented in this table summarize the estimated values of the scales of fluctuation obtained using Approach A (the conventional approach) and the

estimated values obtained using Approach B. The *true* values of the vertical and horizontal scales of fluctuation are included in the table and are used to assess the accuracy achieved in the estimates provided by each method.

The average of the 30 initial estimates of θ_v (i.e. Approach A) is 0.51 m, giving a relative error of about 2% (Table 4). Similar values are obtained when using Approach B: an average θ_v = 0.53 m, giving a relative error of about 5%. In other words, in the vertical direction where data are plentiful, both approaches give accurate results. In the horizontal direction, the results obtained when using Approach B are significantly better than those obtained via the conventional approach. Specifically, when using Approach A the average is θ_h = 3.66 m and the relative error is about 27%, whereas, when using Approach B, the average is θ_h = 3.99 m and the relative error is now about 20% (Table 4). The decrease in relative error from 27% (Approach A) to 20% (Approach B) is quite significant given the fundamental problems with estimating a scale of fluctuation using a relatively large sampling length and few sample points.

The results of Table 4 show that the conventional approach provides reasonable initial estimates for θ_v and θ_h. Indeed, the values obtained for the vertical scale of fluctuation are extremely successful for both approaches, due to the large amount of data available for the calculation of θ_v. However, some improvement is obtained with Approach B in the horizontal direction, when fewer data are available. The better match to the *true* horizontal scale of fluctuation may be due to the algorithm using the available site information more effectively (Lloret-Cabot et al., 2012). By constraining the random fields, at the locations of the actual CPT measurements, improved approximations of the q_c values in between the CPT locations are possible, resulting in a

more realistic estimation of the horizontal correlation function and a better estimation of the average θ_h (Table 4).

5. Conclusions

Two approaches for estimating the vertical and horizontal scales of fluctuation have been presented and subsequently applied to a real case study and then to a simulation-based study to assess relative accuracy.

The accuracy of the estimate of the scale of fluctuation is, of course, highly dependent on both the number of data and their spacing. For example, if the true correlation length is 0.1 m and data are spaced by 1.0 m, then an accurate estimate of the correlation length will not be possible. Similarly, if a small number of observations, at any spacing, are available, the estimate will be worse than if a large number of observations are available. In the case study considered in this paper, the vertical scale of fluctuation is expected to be estimated much more accurately than the horizontal scale of fluctuation, due to both the much larger number of observations and the closer spacing of the data in the vertical direction. However, the goal of the paper was to see if different methods could be used to coax a better estimate when samples are scarce.

For the case study, the vertical and horizontal correlation lengths suggested by both approaches are similar. In particular, the estimated values of θ_v are very close for the three sections analysed, suggesting that the variability in the vertical direction is very consistent across the sections considered. This is not the case, however, for the horizontal scale of fluctuation, where each section converges to a significantly different mean value, suggesting that θ_h has different values at each section analysed and/or that the CPTs are not spaced closely enough for an accurate estimation of θ_h.

The simulation-based study suggests that there is not much difference between the two approaches when the sampling distance is small relative to the correlation length, as there are then plenty of data for estimating θ (i.e. in the vertical direction). This confirms the finding in the case study that, for the vertical direction, the conventional approach already provides a reasonable estimate of θ_v, because enough data are already available. However, when the sampling distance is large relative to the correlation length and there are few data values (e.g. in the horizontal direction), the conditional random field approach shows some improvement over the conventional approach, with the horizontal correlation length being somewhat closer to the *true* value. The difference is quite significant, with the relative error decreasing from 27% in the case of the conventional approach to 20% in the case of the conditional random field approach, which is a quite remarkable improvement given the fundamental problems with estimating a scale of fluctuation using a relatively large sampling length and few sample points.

The results of this study indicate that, for most practical purposes, the conventional approach to estimating the spatial correlation length is adequate, especially when large amounts of data are available. However, when some improvement is desired, particularly when data are scarce, the use of conditional random fields is worth considering.

Acknowledgements

The authors gratefully acknowledge the support provided by the EU FP7 programme under the project 'Geo-Install' (PIAP-GA-2009-230638).

6. References

Baecher, G.B. and Christian, J.T., 2003. *Reliability and statistics in geotechnical engineering*. John Wiley & Sons, West Sussex, England.

Campanella, R.G., Wickremesinghe, D. and Robertson, P.K., 1987. Statistical treatment of cone penetrometer test data. *Proc. 5th Int. Conf. Application of Statistics and Probability.* Vancouver, 1011–1019.

Cassidy, M.J., Uzielli, M. and Tian, Y., 2013. Probabilistic combined loading failure envelopes of a strip footing on spatially variable soil. *Computers and Geotechnics*, 49, 191–205.

Cressie, N., 1990. The origins of Kriging. *Mathematical Geology*, 22 (3), 239–252.

Dasaka, S.M. and Zhang, L.M., 2012. Spatial variability of in situ weathered soil. *Géotechnique*, 62 (5), 375–384.

DeGroot, D.J. and Baecher, G.B., 1993. Estimating auto-covariance of in-situ soil properties. *ASCE Journal of Geotechnical Engineering*, 119 (1), 147–166.

Eijnden, A.P. van den and Hicks, M.A., 2011. Conditional simulation for characterizing the spatial variability of sand state. *Proc. 2nd Int. Symp. Comp. Geomech.*, Dubrovnik, 288–296.

Fenton, G.A., 1999. Estimation for stochastic soil models. *ASCE Journal of Geotechnical and Geoenvironmental Engineering*, 125 (6), 470-485.

Fenton, G.A. and Griffiths, D.V., 2003. Bearing capacity prediction of spatially random $c - \phi$ soils, *Canadian Geotechnical Journal*, 40 (1), 54–65.

Fenton, G.A. and Griffiths, D.V., 2005. Three-dimensional probabilistic foundation settlement, *ASCE Journal of Geotechnical and Geoenvironmental Engineering*, 131 (2), 232–239.

Fenton, G.A. and Griffiths, D.V., 2008. *Risk assessment in geotechnical engineering*. John Wiley & Sons, New Jersey, USA.

Fenton, G.A. and Vanmarcke, E.H., 1990. Simulation of random fields via local average subdivision. *ASCE Journal of Engineering Mechanics*, 116 (8), 1733–1749.

Griffiths, D.V., Huang J.S. and Fenton, G.A., 2009. Influence of spatial variability on slope reliability using 2-D random fields. *ASCE Journal of Geotechnical and Geoenvironmental Engineering*, 135 (10), 1367–1378.

Hicks, M.A. and Onisiphorou, C., 2005. Stochastic evaluation of static liquefaction in a predominantly dilative sand fill. *Géotechnique*, 55 (2), 123–133.

Hicks, M.A. and Samy, K., 2002. Influence of heterogeneity on undrained clay slope stability. *Quarterly Journal of Engineering Geology and Hydrogeology*, 35 (1), 41–49.

Hicks, M.A. and Smith, I.M., 1988. Class A prediction of Arctic caisson performance. *Géotechnique*, 38 (4), 589–612.

Hicks, M.A. and Spencer, W.A., 2010. Influence of heterogeneity on the reliability and failure of a long 3D slope. *Computers and Geotechnics*, 37 (7–8), 948–955.

Jaksa, M.B., Kaggwa, W.S. and Brooker, P.I., 1993. Geostatistical modelling of the undrained shear strength of stiff, overconsolidated, clay. *Proc. Conf. Probabilistic Methods in Geotechnical Engineering*, Canberra, 185–194.

Journel, A.G. and Huijbregts, Ch.J., 1978. *Mining Geostatistics*. Academic Press, New York.

Kim, H-K. and Santamarina, J.C., 2008. Spatial variability: drained and undrained deviatoric load response. *Géotechnique*, 58 (10), 805–814.

Krige, D.G., 1951. A statistical approach to some basic mine valuation problems on Witwatersrand. *Journal of the Chemical, Metallurgical and Mining Society of South Africa*, 52 (6), 119–139.

Lloret, M., Hicks, M.A. and Wong, S.Y., 2012. Soil characterisation of an artificial island accounting for heterogeneity. *Proc. Conf. Geocongress 2012*, San Francisco, 2816–2825.

Lloret-Cabot, M., Hicks, M.A. and van den Eijnden A.P., 2012 Investigation of the reduction in uncertainty due to soil variability when conditioning a random field using Kriging. *Géotechnique letters*, 2 (3), 123–127.

Lloret-Cabot, M., Hicks, M.A. and Nuttall, J.D., 2013. Investigating the scales of fluctuation of an artificial sand island. *Proc. Int. Conf. Geotechnical Installations in Geotechnical Engineering 2013*, Rotterdam, 192–197.

Phoon, K-K., and Kulhawy, F.H., 1999. Characterization of geotechnical variability, *Canadian Geotechnical Journal*, 36 (4), 612–624.

Uzielli, M., Vannucchi, G. and Phoon, K-K., 2005. Random field characterisation of stress-normalised cone penetration testing parameters. *Géotechnique*, 55 (1), 3–20.

Vanmarcke, E.H., 1977. Probabilistic modeling of soil profiles, *ASCE Journal of the Geotechnical Engineering*, 103 (11), 1227–1246.

Vanmarcke, E.H., 1984. *Random Fields: Analysis and Synthesis*. The MIT Press, Cambridge, Massachusetts.

Wackernagel, H., 2003. *Multivariate geostatistics: An introduction with applications*. Springer, Germany.

Wickremesinghe, D. and Campanella, R.G., 1993. Scale of fluctuation as a descriptor of soil variability. *Proc. Conf. Probabilistic Methods in Geotechnical Engineering*, Canberra, 233–239.

Wong, S.Y., 2004. *Stochastic characterisation and reliability of saturated soils*. PhD thesis, University of Manchester, UK.

Zhang, L.L., Zhang, L.M. and Tang, W.H., 2008. Similarity of soil variability in centrifuge models, *Canadian Geotechnical Journal*, 45 (8), 1118–1129.

Table 1. Some common correlation models.

Table 2. Cone tip resistance statistics.

Table 3. Estimated values of the scales of fluctuation.

Table 4. Comparing estimated values of θ using the two approaches.

Figure 1. Test site: (a) side view sketch of Tarsuit P-45 core and berm (not to scale); (b) plan view of CPT locations used.

Figure 2. CPT tip resistance data, including the average linear mean trend lines: (a) section AA'; (b) section BB'; (c) section CC'.

Figure 3. . Histograms of normalized de-trended tip resistance: (a) section AA'; (b) section BB'; (c) section CC'.

Figure 4. Estimated values of the vertical scale of fluctuation when using Approach A: (a) section AA'; (b) section BB'; (c) section CC'.

Figure 5. Estimated values of the horizontal scale of fluctuation when using Approach A: (a) section AA'; (b) section BB'; (c) section CC'.

Figure 6. Typical realization of a conditional random field of normalized de-trended tip resistance, for a 2-D section of the test site: (a) section AA'; (b) section BB'; (c) section CC'.

Figure 7. Estimated values of the vertical scale of fluctuation when using Approach B: (a) section AA'; (b) section BB'; (c) section CC'.

Figure 8. Estimated values of the horizontal scale of fluctuation when using Approach B: (a) section AA'; (b) section BB'; (c) section CC'.

Table 1. Some common correlation models.

Correlation model	**Expression**
Gaussian	$\rho(\tau) = \exp\left\{-\pi\left(\frac{\lvert\tau\rvert}{\theta}\right)^2\right\}$
Triangular	$\rho(\tau) = \begin{cases} 1-\frac{\lvert\tau\rvert}{\theta} & \text{if } \lvert\tau\rvert \le \theta \\ 0 & \text{if } \lvert\tau\rvert > \theta \end{cases}$
Spherical	$\rho(\tau) = \begin{cases} 1-1.5\left\lvert\frac{\tau}{\theta}\right\rvert+0.5\left\lvert\frac{\tau}{\theta}\right\rvert^3 & \text{if } \lvert\tau\rvert \le \theta \\ 0 & \text{if } \lvert\tau\rvert > \theta \end{cases}$
Markov	$\rho(\tau) = \exp\left\{\frac{-2\lvert\tau\rvert}{\theta}\right\}$

Table 2. Cone tip resistance statistics.

Property	**Range**	**Mean value**
Section AA' (7 CPTs)		
Mean (μ): MPa	3.00-5.55	3.85
Standard deviation (σ): MPa	0.71-3.01	1.50
Standard deviation (σ_{res}): MPa (trend removed)	0.69-2.37	1.35
Slope of the linear depth-trend (a_{trend}): MPa/m	0.11-1.18	0.36
Intercept of the linear depth trend (b_{trend}): MPa	1.09-3.72	2.48
Section BB' (6 CPTs)		
Mean (μ): MPa	2.70-4.55	3.58
Standard deviation (σ): MPa	0.40-1.28	0.85
Standard deviation (σ_{res}): MPa (trend removed)	0.39-1.01	0.55
Slope of the linear depth-trend (a_{trend}): MPa/m	0.04-0.68	0.39
Intercept of the linear depth trend (b_{trend}): MPa	1.20-2.72	2.06
Section CC' (5 CPTs)		
Mean (μ): MPa	3.37-3.86	3.59
Standard deviation (σ): MPa	0.75-1.68	1.29
Standard deviation (σ_{res}): MPa (trend removed)	0.51-1.51	0.85
Slope of the linear depth-trend (a_{trend}): MPa/m	0.33-0.84	0.58
Intercept of the linear depth trend (b_{trend}): MPa	0.62-2.31	1.36

Table 3. Estimated values of the scales of fluctuation.

Property	**Approach A**	**Approach B**
Section AA' (7 CPTs)		
Vertical scale of fluctuation (θ_v): m	0.42	0.41
Horizontal scale of fluctuation (θ_h): m	1.69	1.82
Section BB' (6 CPTs)		
Vertical scale of fluctuation (θ_v): m	0.42	0.42
Horizontal scale of fluctuation (θ_h): m	5.07	5.60
Section CC' (5 CPTs)		
Vertical scale of fluctuation (θ_v): m	0.44	0.40
Horizontal scale of fluctuation (θ_h): m	13.69	15.86

Table 4. Comparing estimated values of θ using the two approaches.

	True values		**Approach A**		**Approach B**	
	θ_v (m)	θ_h (m)	$\theta_{v,0}$ (m)	$\theta_{h,0}$ (m)	$\theta_{v,j}$ (m)	$\theta_{h,j}$ (m)
Mean (μ): m	0.5	5	0.51	3.66	0.53	3.99
Relative error	-	-	2%	27%	5%	20%

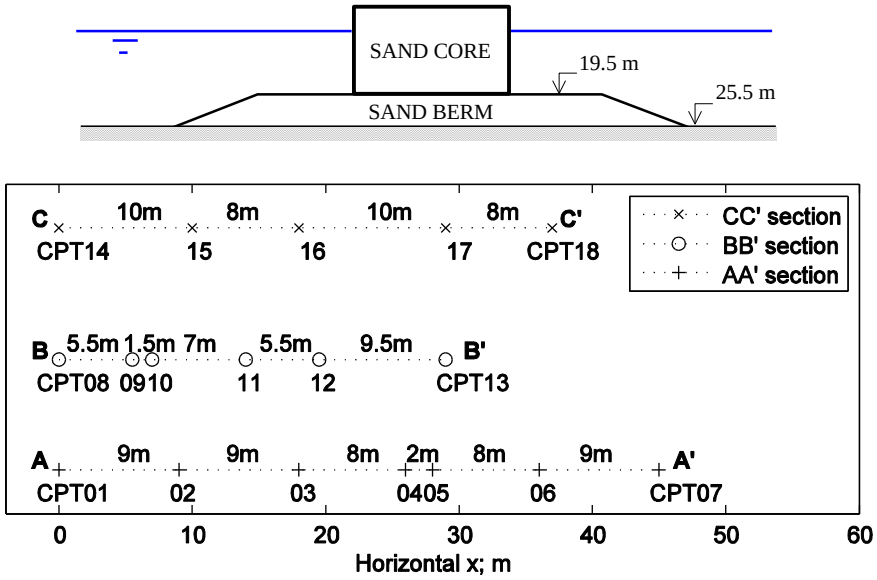

Figure 1. Test site: (a) side view sketch of Tarsuit P-45 core and berm (not to scale); (b) plan view of CPT locations used.

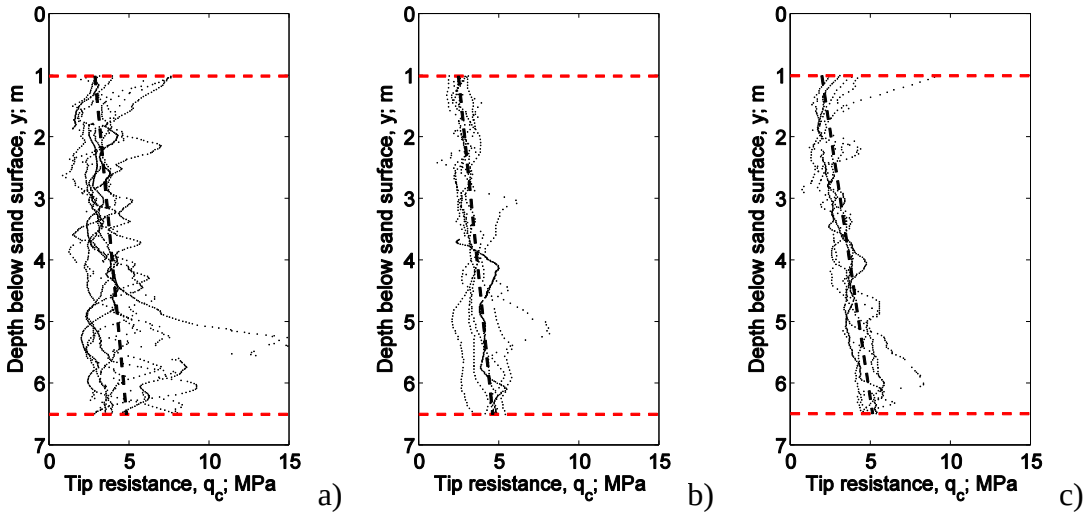

Figure 2. CPT tip resistance data, including the average linear mean trend lines: (a) section AA'; (b) section BB'; (c) section CC'.

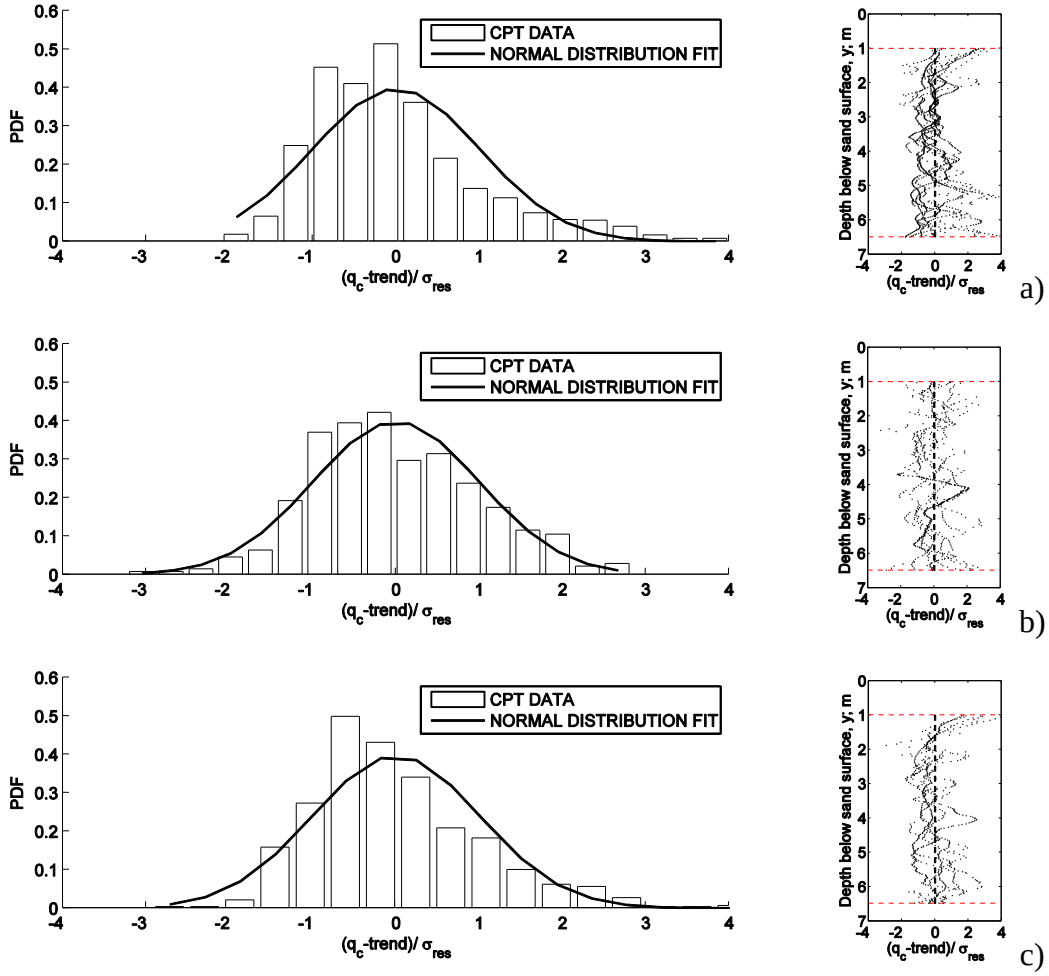

Figure 3. Histograms of normalized de-trended tip resistance: (a) section AA'; (b) section BB'; (c) section CC'.

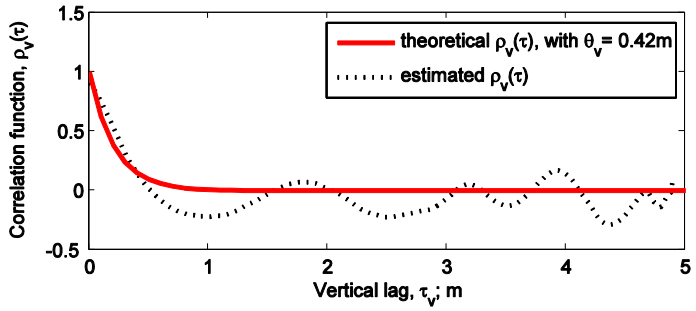

a)

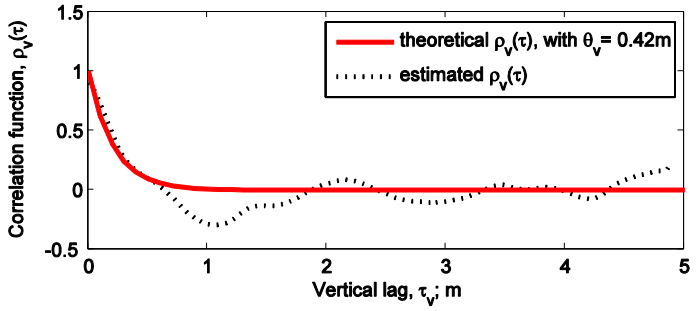

b)

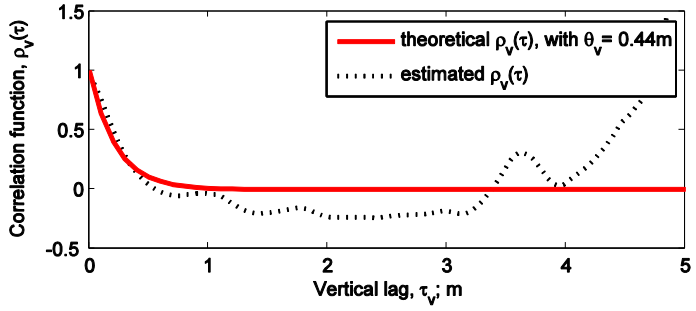

c)

Figure 4. Estimated values of the vertical scale of fluctuation when using Approach A: (a) section AA'; (b) section BB'; (c) section CC'.

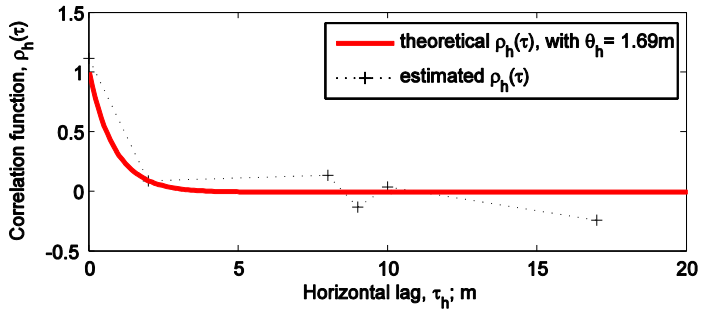

a)

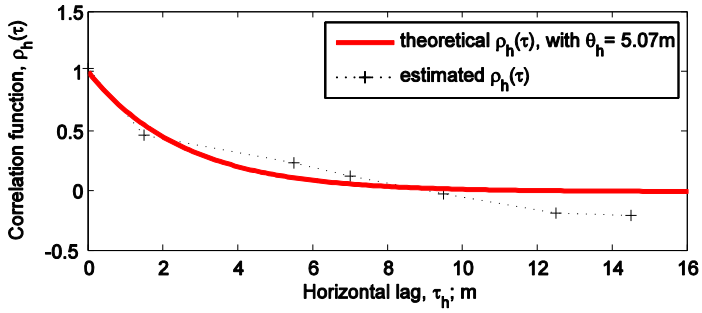

b)

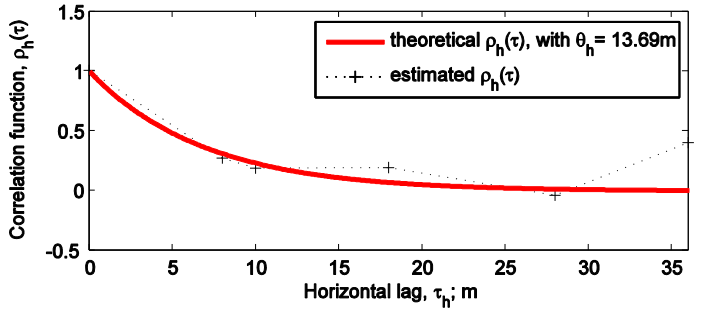

c)

Figure 5. Estimated values of the horizontal scale of fluctuation when using Approach A: (a) section AA'; (b) section BB'; (c) section CC'.

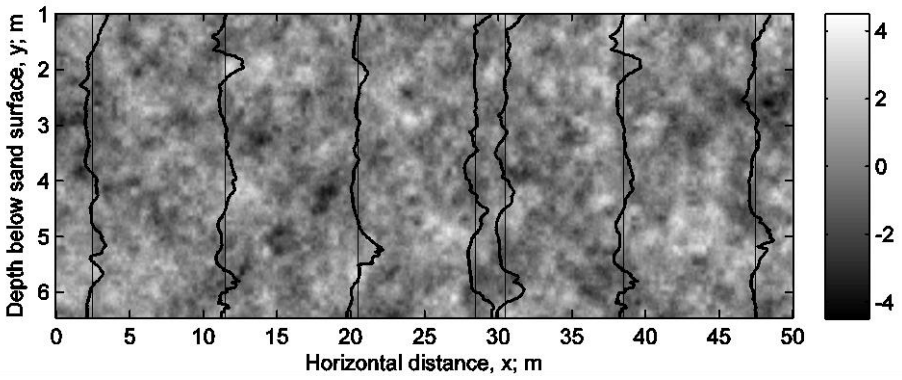

a)

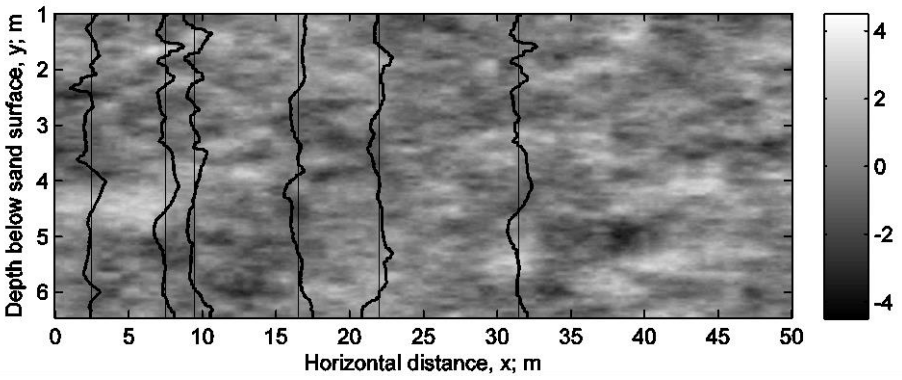

b)

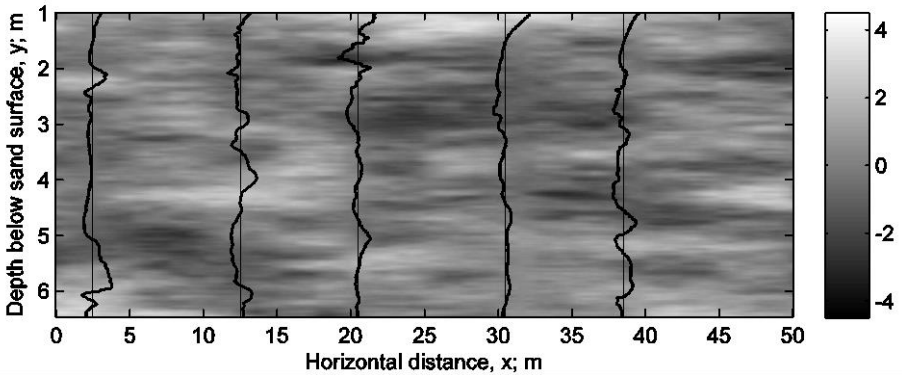

c)

Figure 6. Typical realization of a conditional random field of normalized de-trended tip resistance, for a 2-D section of the test site: (a) section AA'; (b) section BB'; (c) section CC'.

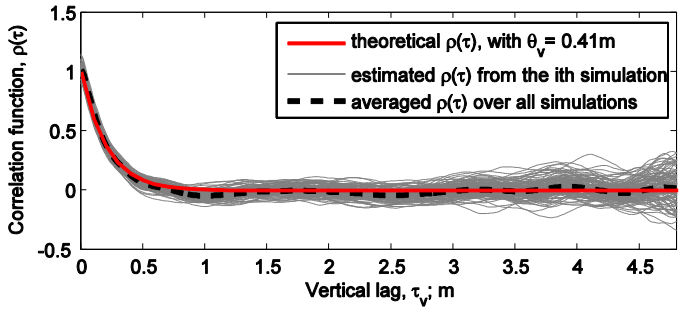

a)

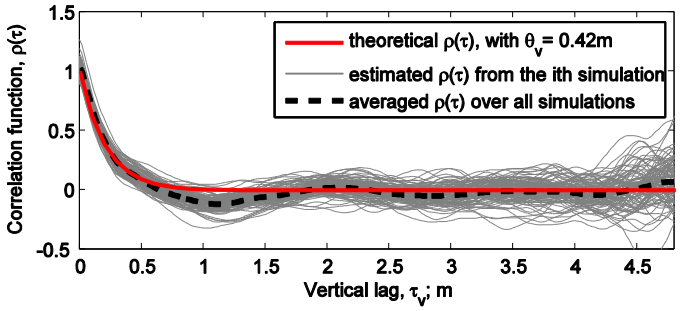

b)

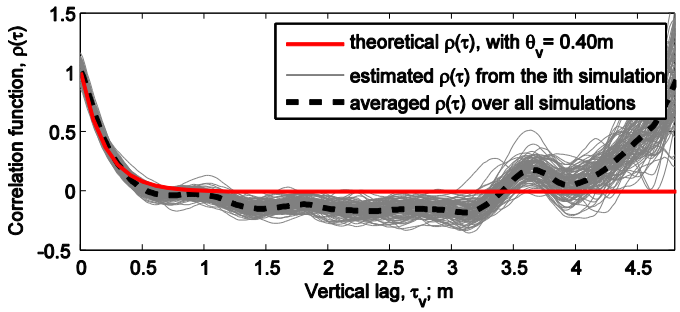

c)

Figure 7. Estimated values of the vertical scale of fluctuation when using Approach B: (a) section AA'; (b) section BB'; (c) section CC'.

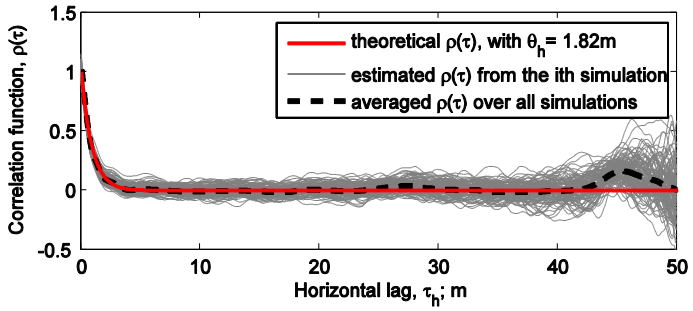

a)

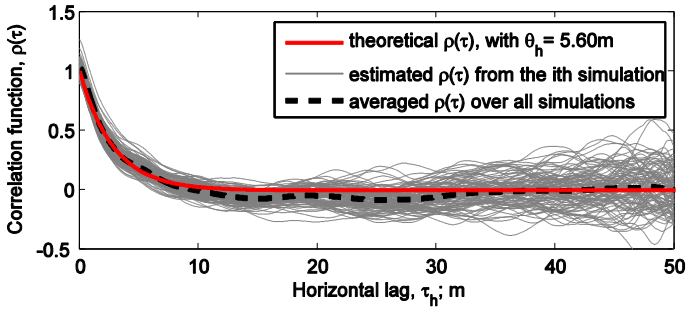

b)

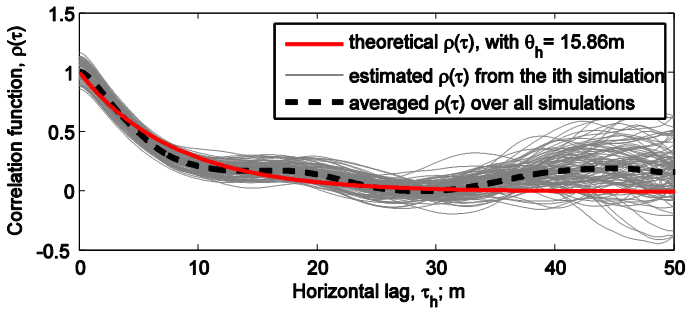

c)

Figure 8. Estimated values of the horizontal scale of fluctuation when using Approach B: (a) section AA'; (b) section BB'; (c) section CC'.